Building Technologies & Urban Systems Division
Energy Technologies Area
Lawrence Berkeley National Laboratory

Development of high-fidelity air handling unit fault models for FDD innovation: lessons learned and recommendations

Armando Casillas[1], Yimin Chen[1], Jessica Granderson[1], Guanjing Lin[2], Zhelun Chen[1], Jin Wen[3] and Sen Huang[4]

[1]Lawrence Berkeley National Laboratory, [2]Tsinghua Shenzhen International Graduate School, Tsinghua University, [3]Department of Civil Architectural and Environmental Engineering, Drexel University, [4]Oak Ridge National Laboratory

Energy Technologies Area
2024

doi.org/10.1080/19401493.2024.2382757

This work was supported by the Assistant Secretary for Energy Efficiency and Renewable Energy, Building Technologies Office, of the US Department of Energy under Contract No. DE-AC02-05CH11231.

Disclaimer:

Journal of Building Performance Simulation

ISSN: (Print) (Online) Journal homepage: www.tandfonline.com/journals/tbps20

Development of high-fidelity air handling unit fault models for FDD innovation: lessons learned and recommendations

Armando Casillas, Yimin Chen, Jessica Granderson, Guanjing Lin, Zhelun Chen, Jin Wen & Sen Huang

To cite this article: Armando Casillas, Yimin Chen, Jessica Granderson, Guanjing Lin, Zhelun Chen, Jin Wen & Sen Huang (2024) Development of high-fidelity air handling unit fault models for FDD innovation: lessons learned and recommendations, Journal of Building Performance Simulation, 17:5, 615-630, DOI: 10.1080/19401493.2024.2382757

To link to this article: https://doi.org/10.1080/19401493.2024.2382757

JOURNAL OF BUILDING PERFORMANCE SIMULATION
2024, VOL. 17, NO. 5, 615–630
https://doi.org/10.1080/19401493.2024.2382757

Development of high-fidelity air handling unit fault models for FDD innovation: lessons learned and recommendations

Armando Casillas[a], Yimin Chen[a], Jessica Granderson[a], Guanjing Lin[b], Zhelun Chen [a], Jin Wen[c] and Sen Huang[d]

[a]Lawrence Berkeley National Laboratory, Environmental Energy Technologies Division, Building Technology and Urban Systems Department, Berkeley, CA, USA; [b]Tsinghua Shenzhen International Graduate School, Tsinghua University, Nanshan, Shenzhen, People's Republic of China; [c]Department of Civil, Architectural and Environmental Engineering, Drexel University, Philadelphia, PA, USA; [d]Oak Ridge National Laboratory, Oak Ridge, TN, USA

ABSTRACT

Interest in automated building analytics, including fault detection and diagnostics has been increasing; however, developers of these solutions have lacked access to ground-truth-validated data across a wide range of weather conditions for algorithm development and performance assessment. This study presents the development, and validation of faulted and fault-free models for air handling units (AHUs) – a common HVAC system design. Detailed models for the single-duct AHU (Modelica) and dual-duct AHU (HVACSIM+) were used to conduct annual simulations, for common sensor, mechanical, and control sequence faults. We report lessons learned during the efforts, including challenges and insights regarding how these simulation models, typically used for design applications, can be purposed to accurately reflect real-world system operational behaviours. Finally, we highlight considerations for researchers and FDD developers who may wish to leverage this dataset to assess the performance of their algorithms, and evolving performance of FDD solutions over time.

ARTICLE HISTORY
Received 17 January 2024
Accepted 16 July 2024

KEYWORDS
Fault detection and diagnostics; HVAC modelling; Modelica; HVACSIM+; controls; fault modelling

1. Introduction and background

As building data becomes more readily available, and as the budding field of data science and analytics comes to buildings, fault detection and diagnostics (FDD) is of increasing relevance to the research and product development communities. A primary method of improving building controls and operational efficiency is through algorithms developed to perform automated FDD, which uses building data to identify the presence of faults and potentially isolate root causes. Estimated energy use reduction from these improvements has been estimated at an average of 29%, which accounts for approximately 5% of overall national energy consumption (Fernandez et al. 2017). Practically, building owners and operators have already leveraged the benefits of AFDD technology, using it to enable median whole-building portfolio savings of 9% (Kramer et al. 2020).

Development of FDD for air distribution subsystems, including hydronic air handling units (AHU) systems, for example, are presented in a number of studies dating back decades (Bushby and Park, 2001; House, Vaezi-Nejad, and Whitcomb 2001; Schein and Bushby 2006). Since then, a diversity of techniques have been developed for FDD in AHU systems, spanning analytical-based physical or grey box models, data-driven approaches, and knowledge-based heuristic approaches (Liao et al. 2021; Wu and Sun 2012; Yu, Woradechjumroen, and Yu 2014), and developers continuously strive to develop improved algorithms. A persistent challenge, however, has been the lack of common datasets and test methods to benchmark the performance accuracy of FDD methods, and gauge improvement of these tools over time. Lin et al. (2020) most recently developed a test and benchmarking framework for FDD algorithm performance, demonstrating a growing need for HVAC fault datasets that can be used to further determine the accuracy and effectiveness of FDD algorithms. HVAC performance datasets have been developed before in the form of ASHRAE's RP1312 fault dataset (Li and Wen, 2010; Li et al. 2010). ASHRAE Project RP-1312 data is the resulting dataset from a series of experiments that were performed on two multi-zone variable air volume (VAV) AHUs (AHU-A and AHU-B) with the same configuration running simultaneously. This experiment yielded fault-free and faulty datasets with ground-truth information for each fault case as well as an understanding of the resulting behaviour for each fault. In addition, ASHRAE Project RP-1312 created a dynamic simulation testbed developed by HVACSIM+ to evaluate AHU's

CONTACT Armando Casillas acasillas@lbl.gov

operational performance. Additionally, Wen et al. (2015) further developed dynamic models for the secondary systems including fan coil units, fan power units, and dual-duct systems, using HVACSIM+ (Wen et al. 2015). The models were used to create fault operation data sets, which contained data in a few days for three operational seasons. This dataset has been leveraged by a number of FDD studies (Montazeri and Kargar 2020; Yan et al 2016; Yun, Hong, and Seo 2021; Zhong et al 2019). Further work was initiated to fill this gap with the introduction of an open-sourced dataset for FDD evaluation purposes (Granderson et al. 2020), which introduced a first-of-its-kind public dataset with ground-truth data on the presence and absence of faults for multiple HVAC systems, including a limited number of fault datasets from a simulated single-duct AHU (SDAHU) system.

While simulation models have commonly been used for design applications, their use in operational analytics and control applications has largely been limited to research as opposed to practice. For example, Granderson et al (2017) employed a calibrated physics-based modelica model for FDD applications by detecting wide deviations between measured and modelled COP, while Andriamamonjy et al (2018) developed a model-based FDD toolchain for an AHU built through a building information model. Although system-level energy and controls modelling such as that offered in Modelica, HVACSim+ and Spawn of Energy Plus hold promise for expanded utilization for operational applications, it remains challenging to configure them in a way that accurately reflects system operation across a variety of configurations, sequences of operation, loads, and seasons.

As established, there is a need for more fault datasets with established ground-truth information, a gap that high-fidelity models are starting to fill. However, there are a limited number of studies that document the ability of these models to emulate 24-hr behaviour in real systems, including studies by (Granderson et al. 2020), which were limited to 18 fault cases, and Wen et al. (2015). This research makes three primary contributions. (1) Development of the largest public AHU fault data set including annual 8760-hour datasets covering 75 fault cases, building upon initially limited datasets presented in Granderson et al. (2020), which was limited to 18 fault cases, and Wen et al. (2015) which presented merely 1–2 days worth of data per fault case. Specifically, we will be covering two configurations of this system in single-duct and dual-duct AHU. The data set consists of high-resolution, simulated time series HVAC operational data (e.g. temperatures, pressures, control signals, component status, etc.) under a diversity of operating and weather conditions, combined with information on the presence and absence of faults and their associated intensity. (2) Application of a structured quality assurance assessment protocol to ensure valid operational data and ground truth (Casillas et al. 2020). (3) Identification of existing gaps and best practices in employing high-fidelity modelling to reflect real-world system behaviours. A clear articulation of these gaps can enable HVAC system model developers and FDD algorithm developers to avoid mistakes and inaccuracies in operations-focused uses of system-level simulation models and can inform the modelling community as to useful contributions to extend the modelling state of art and practice. In the remainder of this article, section 2 describes the study methodology, providing model descriptions and the development of fault scenarios. Section 3 presents the modelling results for both single and dual-duct systems across multiple seasons and section 4 addresses the challenges, gaps and lessons learned from employing these models to emulate real-world existing HVAC systems. Concluding remarks and potential avenues for future research are outlined in section 5.

2. Methods

Two types of AHUs, i.e. the SDAHU and the dual-duct AHU (DDAHU) were designed based on ASHRAE Handbook schematics and descriptions (ASHRAE 2020) andsimulated based on the various simulation software tools such as Modelica, EnergyPlus and HVACSIM+ as described in previous studies (Huang et al. 2018; Wen et al. 2015). For each type of fault, the fault was injected into the system and the simulation was performed to output one-year (i.e. 365 days) fault-inclusive data. Consequently, the fault-inclusive data cover all operating conditions of the AHUs under one-year time scope. In this section, we illustrate the simulation method for each type of equipment as well as the complete list of points included in our simulation output in Table 1, with corresponding abbreviations found in Figures 1 and 2.

2.1. Single-duct AHU (SD-AHU)

The SDAHU model was developed in the Modelica language by developers at PNNL, based on model components available in open-source Modelica libraries such as the Modelica Buildings and IBPSA libraries. Modelica is an equation-based, objective-oriented modelling language for complex dynamic systems. In order to capture the building's thermal response a reference commercial building model from EnergyPlus (Deru et al. 2011) was integrated. The data exchange between the EnergyPlus input data file (IDF) model and the Modelica system model was handled by a co-simulation framework,

Table 1. Abbreviations and definitions for points included in SDAHU and DDAHU model.

Data point abbreviation	Description
SYS_CTL	System control mode
OA_CFM	Outdoor air flow rate
OA_DMPR	Outdoor air damper position signal
OA_DMPR_DM	Outdoor air damper control signal (command)
OA_HUMD	Outdoor air humidity
OA_TEMP	Outdoor air temperature
MA_TEMP	Mixed air temperature
SA_TEMP	Supply air temperature
SA_TEMPSPT	Supply air temperature set point
SF_SPD_DM	Supply air fan status
SA_CFM	Supply volumetric airflow
SF_CS	Supply air fan speed control signal
SF_SPD	Supply air fan speed position
SF_WAT	Supply air fan power
SA_SP	Supply air duct static pressure
SA_SPSPT	Supply air duct static pressure set point
RA_CFM	Return air flow rate (sum of all zones returns)
RA_DMPR	Return air damper position signal
RA_DMPR_DM	Return air damper control signal
RA_HUMD	Return air humidity
RA_TEMP	Return air temperature
RF_DP	Return fan differential pressure
RF_SPD	Return fan VFD speed
RF_WAT	Return fan power
EA_DMPR	Exhaust air damper position signal
EA_DMPR_DM	Exhaust air damper control signal (command)
HSA_SPSPT	Hot deck supply air duct static pressure setpoint
HSA_SP	Hot deck supply air duct static pressure
HSA_HUMD	Hot deck supply air humidity
HSA_CFM	Hot deck supply air flow rate
HSA_TEMPSPT	Hot deck supply air temperature setpoint
HSA_TEMP	Hot deck supply air temperature
HSF_CS	Hot deck supply fan status (on/off)**
HSF_DP	Hot deck supply fan differential pressure
HSF_SPD	Hot deck supply fan VFD speed
HSF_WAT	Hot deck supply fan power
CSA_SPSPT	Cold deck supply air duct static pressure setpoint
CSA_SP	Cold deck supply air duct static pressure
CSA_HUMD	Cold deck supply air humidity
CSA_CFM	Cold deck supply air flow rate
CSA_TEMPSPT	Cold deck supply air temperature setpoint
CSA_TEMP	Cold deck supply air temperature
CSF_CS	Cold deck supply fan status (On/Off)
CSF_DP	Cold deck supply fan differential pressure
CSF_SPD	Cold deck supply fan VFD speed
CSF_WAT	Cold deck supply fan power
HWC_DAT	Heating water coil discharge air temperature
HWC_EWT	Heating water coil entering water temperature
HWC_LWT	Heating water coil leaving water temperature
HWC_MWT	Heating water coil mixed water temperature
HWC_VLV	Heating water coil valve position signal
HWC_VLV_DM	Heating water coil valve control signal
HWP_GPMC	Heating water pump water flow rate through coil
HWP_GPMT	Heating water pump total water flow rate
CHWC_DAT	Cooling coil discharge air temperature
RM_TEMP	Room temperature
VAV_DAT	Mixing box discharge air temperature
VAV_SP_C	Mixing box cold deck dynamic pressure
VAV_SP_H	Mixing box hot deck dynamic pressure
VAV_DMPR_C	Mixing box cold deck control signal
VAV_DMPR_H	Mixing box hot deck control signal
VAVCFM_C_DM	Mixing box cold deck demanded air flow rate
VAVCFM_H_DM	Mixing box hot deck demanded air flow rate
VAVCFM_C	Mixing box cold deck air flow rate
VAVCFM_H	Mixing box hot deck air flow rate
VAVCFM_T	Mixing box total air flow rate
VAV_EAT_C	Mixing box cold deck entering air temperature
VAV_EAT_H	Mixing box hot deck entering air temperature

exporting the IDF file as a functional mockup unit, analogous to the methods in Huang et al. (2021). In addition to calculating the thermal loads of the space, the IDF file also stores pertinent weather information that is fed into the modelica model, which allows for annual modelling of a building based on a historical weather data set. For this study's purposes, the climate data modelled was that of Chicago, Il. Modelica simulations have a variable simulation time step, which becomes more granular as the solver encounters instances of more computational complexity. The reporting timestep was set to 60 s. The major components of the modelled for the SDAHU, as shown in Figure 1, are the supply air fan with a variable frequency drive (VFD), return fan with a VFD, cooling coil, cooling control valves, outdoor air (OA) and return air (RA) dampers. This model does not include a heating coil or heating coil valve components. The measurement points made available for end users are related to the aforementioned components, including temperature, airflow and static pressure readings, temperature and pressure setpoints, control signal and positions for actuated components, and speed and power output for motorized components. Further details of this model are described by Huang et al. (2018). The AHU's baseline control sequence is applied from engineering standard best practices (e.g. ASHRAE 90.1) and is detailed below in Table 2. These control parameters and sequences are programmed in the modelica language with control and logic components.

The control loops are mostly concerned with three different components and are based on the occupancy state, as defined by the EnergyPlus IDF occupancy schedule:

(1) Fan speed control determined by occupancy state and static pressure setpoints
(2) Cooling coil valve determined by occupancy state and supply air temperature (SAT) setpoint
(3) Damper positions determined by occupancy state, outdoor air temperature and mixed air temperature setpoint

2.2. Dual-duct AHU (DDAHU) system

The DDAHU system equips two separate supply air ducts as a hot duct and a cold duct, and two supply air fans in each duct to provide desired air circulation and thermal comfort to different zones. In this system, both the heating and cooling coils can operate at the same time. The hot air and the cold air will be mixed with dampers in VAV terminal units at each zone. In this study, the DDAHU system was developed by the HVACSIM+ software tool,

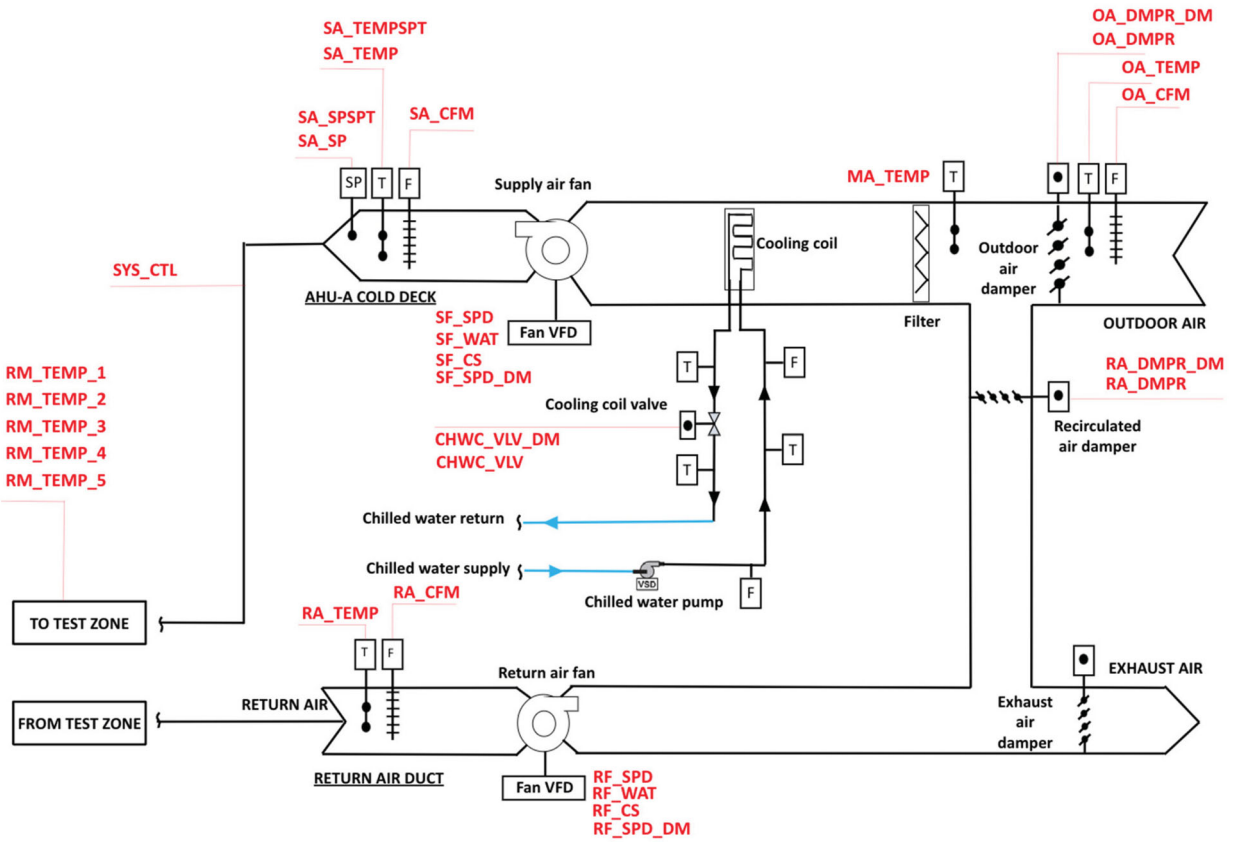

Figure 1. SDAHU diagram with all measurement points denoted.

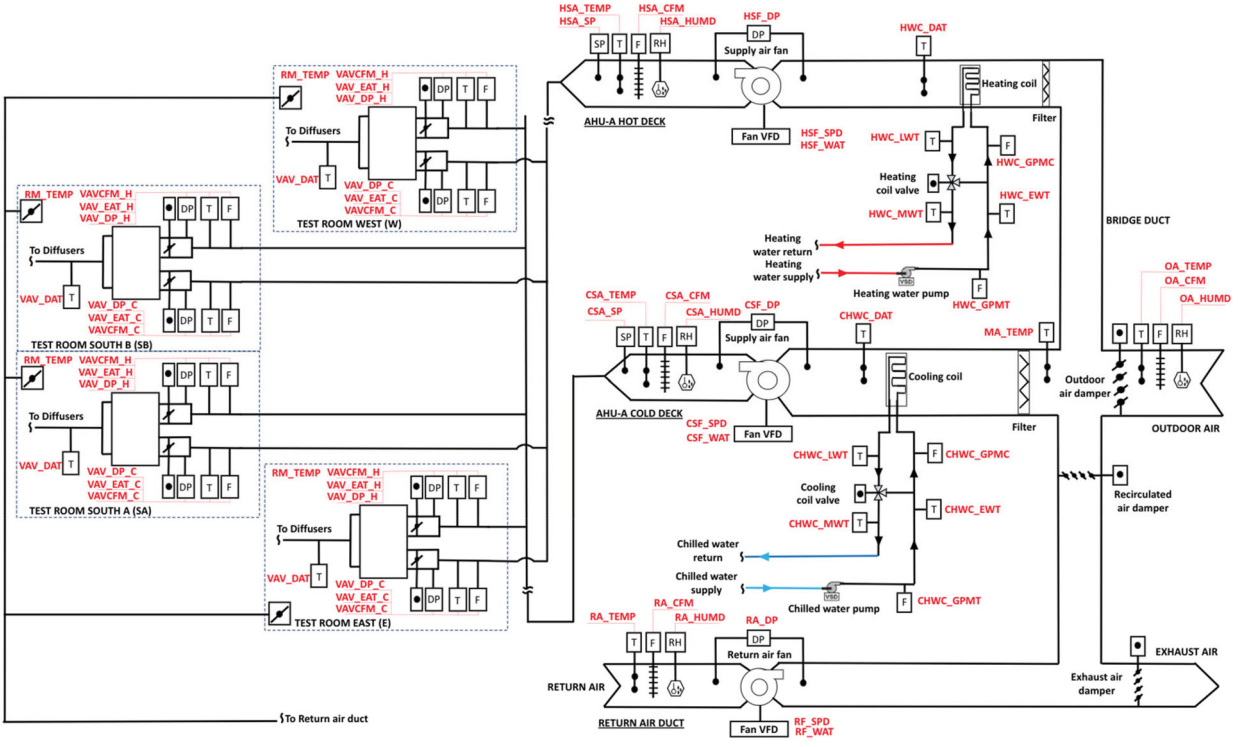

Figure 2. DDAHU diagram with all measurement points denoted.

Table 2. Controls overview for SDAHU and DDAHU models.

Control/operations specification		SDAHU		DDAHU	
		Typical building control baseline	Data source/ references	Typical building control baseline	Data source/ references
System operation mode	Occupied mode	Start HVAC system 2 h ahead of occupancy schedule: • Occupancy schedule (weekday 6:00–22:00) • Cooling setpoint (occupied): 26.7°C (75°F) • Heating setpoint (occupied): 21°C (70°F)	DOE commercial reference building (Deru, et al., 2011)	The system operates following schedule as: occupied hours (Monday – Friday 6:00AM–6:00PM	NIST 10D243 Tools for Evaluating Fault Detection and Diagnostic Methods for HVAC Secondary Systems of a Net Zero Building (Wen et al., 2015)
	Unoccupied mode	Maintain unoccupied heating and cooling setpoint: • Cooling setpoint (unoccupied): 24°C (80°F) • Heating setpoint (unoccupied):15.6°C (60°F)		Unoccupied hours (Monday – Friday 6:00PM – 6:00AM, and Saturday – Sunday 24-hour	
Air handling unit	Supply /return fan control	Fixed static pressure (SP), SP set: 169.2 Pa (0.68 in. w.g.)	Based on testing, air balancing analysis of the given system to meet cooling design condition	Fixed SP, SP setpoint: 398.1 Pa (1.6 in. w.g.)	Based on air balancing analysis of the given system to meet ventilation design and noise control
		Fixed differential speed ratio (10% less) between supply air and return air fan.	Based on engineering practices	The return air fan speed is the same with the supply air fan speed	Based on engineering practices
	Supply air temperature control	Fixed SAT setpoint: 12.7°C (55°F)	Based on engineering practices	Fixed SAT setpoints • Cold deck SAT setpoint: 12.8°C (55°F) • Hot deck SAT setpoint: 32.2°C (90°F)	Based on engineering practices
	Minimum outdoor air control	Fixed minimum OA damper position (10% open) during the occupied hour. Closed during the unoccupied hour.	Based on engineering practices	Summer season: • the economizer mode is disabled, • the OA damper position: 28% openness. Winter and shoulder season: • the economizer mode is enabled • the OA damper position: 45% openness	Based on engineering practices
	Economizer	Fixed dry bulb temp threshold, OA damper engaged from 1°C to 15.6°C (33°F to 60°F), otherwise at minimum position (10%). Damper modulates to hold mixed air temperature of 12.8°C (55°F).	ASHRAE Guideline 36-2021/ASHRAE 90.1-2016	When the OA temperature $<$ 15.6°C (60 °F) and PI controller output is lower than 100, cooling coil valve position is fully closed; the OA damper is adjusted between 0% to 100% open position.	Based on engineering practices

which was developed by the National Institute of Standards and Technology (Clark & May, 1985). The system contains a dual-duct AHU and four associated VAV terminal units, which serve four zones as shown in Figure 2. In the HVACSIM+ simulation platform, various elements such as parts, components and control sequences in an HVAC system can be modelled to create various instance blocks referred to as different 'TYPE' components. Various components can be grouped into 'superblocks' for simultaneous solutions. Consequently, each superblock is a numerically independent subsystem of the overall simulation. Each superblock can independently handle its time evolution and internal solution during the simulation process. In addition, the time step in a superblock is a variable that is automatically and continuously adjusted by a solver subroutine to maintain numerical stability. For this study, the time step was set at 5 s. Further details of this model can be found in Wen et al. (2015).

Before imposing faults on the simulation platform, various simulation settings were determined to ensure the simulation accuracy. The simulation setting includes three parts: (1) control sequence and parameter settings, (2) zone load settings and (3) environment parameter settings. The control sequence includes the operation mode sequence, and individual component control sequences for the fan, dampers, cooling coil valve and heating coil valve, as summarized in Table 2 below. The hourly zone internal load value was set according to Park et al. (1986). The TMY3 weather data for Des Moines, IA, was used as the weather inputs as the system model was developed in Iowa Energy Centre.

2.3. Fault modeling

Three different components were targeted for fault modelling in the SDAHU model: the outdoor air damper, the cooling coil and the temperature sensors. The faults are all implemented by modifying or overriding the baseline control logic of the model. For example, the outdoor air damper stuck fault is implemented by overriding the position of the damper component. The fault imposition methods are summarized in Table 3 below. As an example, for each intensity of the OA damper stuck fault, the fault is imposed by overriding the position of the modelled damper to the predetermined value. The scaled dataset creation is carried out with a parametric simulation Modelica script. This allows for the intensity of each fault to be modelled based on a single value that is passed as a parameter into the fault model component such as 'TwoWayValveStuck' for both the cooling coil valve and OA damper.

In the DDAHU study, a total of 15 types of faults which are commonly studied by academic publications and reported by field engineers on the AHU side were imposed to obtain fault-inclusive operation data (Chen et al. 2021; Roth et al. 2004; Schein and Bushby, 2006; Wang and Xiao 2004; Zhao, Wen, and Wang 2015; Zhao et al. 2017). For hardware faults such as stuck heating and

Table 3. Overview of HVAC fault modelled and imposition method.

Fault	Method of fault imposition	Severities modelled	System
Supply, outdoor air temperature, static pressure sensor bias	Add or subtract constant value from initial sensor reading	−4,−2, 2, 4°C	SDAHU
		−100, −50,50,100 Pa	DDAHU
outdoor air, cooilng/heating damper, cooling/heating coil valve stuck	Automated override of damper position to indicate that damper is stuck. Automated override of coil valve position to indicate that cooling coil valve is stuck.	Damper (0%,10%, 20, 25%, 75%, 100%)	SDAHU
		Valve (0%, 10%, 20%, 25%, 50%, 80%, 100%)	DDAHU
Cooling coil valve leak	Adjusted the minimum coil valve position value when control signal is zero	10%, 25%, 40%, 50%	SDAHU and DDAHU
Cooling/heating coil fouling fault (air side)	Modified fin and tube heat transfer coefficients in the coil component	Minor: 10% airflow resistance increase	DDAHU
		Moderate: 50% airflow resistance increase, 5% heat transfer reduction	
		Severe: 200% airflow resistance increase, 10% heat transfer reduction	
Cooling/heating coil fouling fault (water-side)	Modified fin heat transfer coefficient, tube heat transfer coefficient, and the coil fluid flow resistance in the coil components	Minor: 10% water flow rate and heat transfer heat rate reduction	DDAHU
		Moderate: 30% water flow rate and heat transfer heat rate reduction	
		Severe: 50% water flow rate and heat transfer heat rate reduction	
Cooling/heating control sequence unstable	Changed the absolute value of the proportional band of the cooling and heating control sequences from a properly tuned value of 45.7 to an improper value of −4	Faulted: Increase proportional band until unstable	DDAHU

cooling damper and coil valves, the simulations with multiple severity levels were performed for each type of fault. For the software faults, such as unstable control, the simulations with a single severity level were performed for each type of fault. Consequently, a total of 55 fault simulation cases were carried out in this study, of which the type and severities are listed in Table 3. Each fault case was simulated to generate one year of operation data, which simulates the fault for the duration of the year so that all system's operational conditions can be covered to fully evaluate the measurement sensitivity under various operational conditions.

The symptoms of each fault are detailed below:

The **outdoor air damper stuck fault** is a mechanical fault by nature and will directly affect the AHU's ability to take advantage of outdoor air to maintain supply temperatures while minimizing cooling energy as well its ability to maintain effective supply temperature control. During instances in which the OA damper is stuck above the minimum position and supply air is cooler than the desired setpoint, excess outdoor air may cause the cooling energy to be minimized while dramatically reducing the SAT of the AHU. In the case in which warmer temperatures are seen outdoors, the excess outdoor air will cause more cooling energy to be used, driving the control signal of the OA damper to a minimum while maximizing the cooling coil control signal. Higher than normal supply air temperatures may occur.

A **stuck cooling coil valve** directly affects the AHU's ability to maintain effective supply temperature control. During instances in which the supply air is warmer than desired, the control signal will be driven to 100% due to the inability of the system to maintain cool enough air to the zone level. This will cause higher than normal supply and return air temperatures, and higher overall cooling energy consumed. During instances in which the cooling coil is providing too much cooling, or a supply temperature colder than the setpoint, the control signal will eventually be driven to zero due to the inability of the system to maintain SAT set point. This will ultimately lead to lower than desired supply and return air temperatures and higher overall cooling energy consumed.

A **leaking cooling coil valve** affects the AHU's ability to fully close the cooling coil valve. During instances in which the control signal is driven to a level below the leakage level or to 0, the ground-truth position of the valve will bottom out at the leakage level. This will cause lower than normal supply temperatures during these instances, and higher overall cooling energy consumed. During instances in which the leakage level is higher than the control signal, the fault will behave more like a stuck valve fault.

A **temperature sensor bias fault in the outdoor temperature sensor** would cause an adverse effect on supply temperature control, mainly the modulation of the outdoor air damper according to the economizer control sequence. As the bias becomes more positive (4C), the seemingly higher outdoor air temperature would result in less activity in the economizer control signal, resulting in higher overall cooling energy consumption.

A **temperature sensor bias fault in the supply temperature sensor** would cause an adverse effect on supply temperature control, mainly the modulation of the cooling coil valve to meet the setpoint. As the bias becomes more positive (4C), the seemingly higher supply temperature would result in a higher control signal for added cooling, resulting in higher overall cooling energy consumption, cooler rooms (lower return air temperatures)

Both **the coil fouling air-side fault and water-side fault** would cause several typical symptoms such as decreased water flow rate, increased coil valve position to provide desired cooling/heating capacity and increased or decreased SAT. For example, if the heating coil is severely fouling, the heating water flow will be significantly decreased. In the winter season, this may lead the heating coil valve position to be higher than normal to provide the desired heating. Under some extremely cold weather conditions, the SAT may be lower than normal due to the severe impacts on the heating supply capacity. For the fouling fault types, three fault severity levels (minor, moderate and severe) were imposed by decreasing the fluid flow rate and the decreasing heat transfer rate.

Both **cooling and heating control sequence faults occur in the valve controllers.** The control sequence fault causes the valve position to be unstable and consequently causes SAT to be fluctuate. The fault was imposed by changing the absolute value of the proportional band setting from 45.7 to −4 in the PID controller until the valve operation was unstable.

2.4. Model data validation process

The scale generation of these annual datasets was preceded by a methodical data validation and ground-truth assessment protocol as laid out in Casillas et al (2020) and in Figure 3. This process allowed for the iterative development of these AHU models in order to ensure they exhibited the expected behaviours under fault-free and faulty conditions across all seasons and weather conditions. The process begins with the development of the physical model while also specifying and programming the control sequence. After weekly simulations are completed for each season, the simulation data is validated against the intended control sequence to determine all

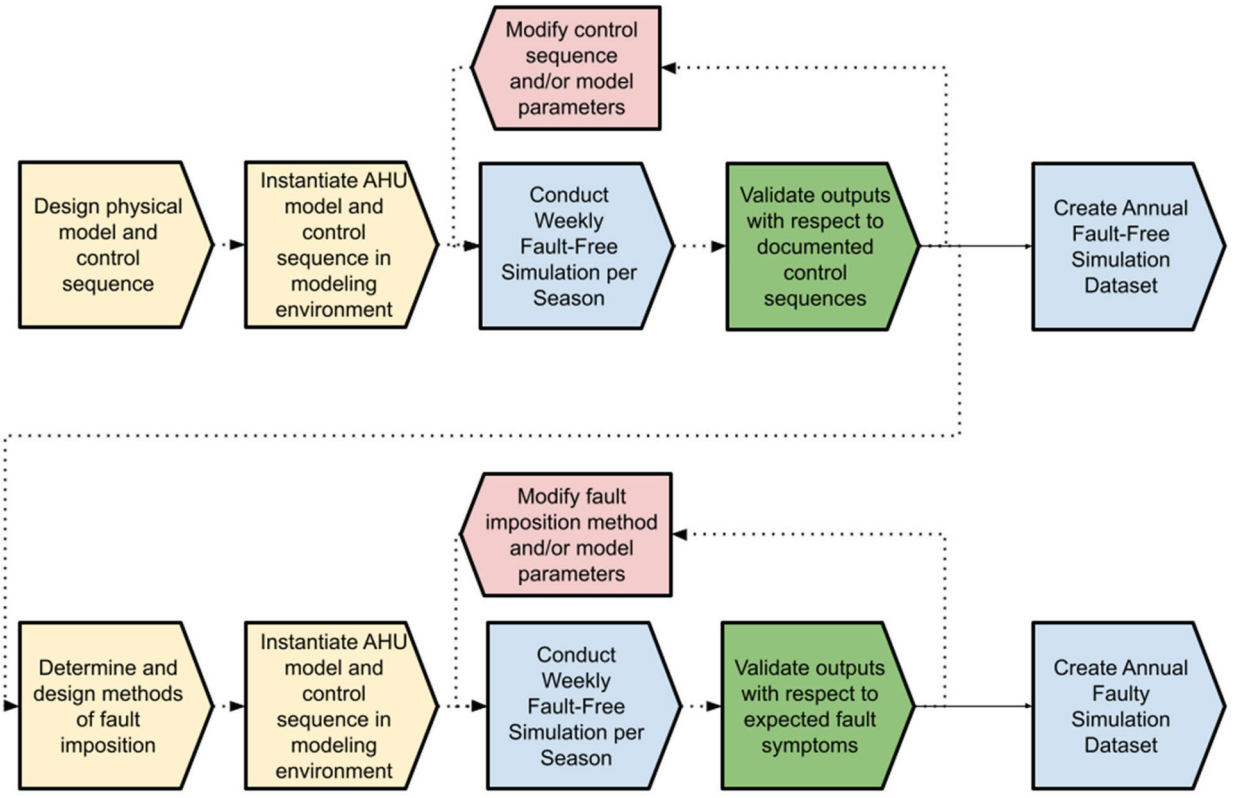

Figure 3. Workflow diagram for scaled fault-free and faulted dataset generation.

systems are behaving as expected. The application of the validation protocol enabled the appropriate changes to the model design and parameters to ensure high-quality data. Most of the issues described in this study's discussion were encountered during this validation step. Changes to the models include modifications to component sizing, control sequences, and methods of fault imposition.

3. Results

The annual fault cases are modelled in their respective tools, then validated to ensure the fault behaviours are as expected based on our knowledge-based approach. The ability to conduct annual fault simulation is one of the most valuable contributions since this allows us to observe the fault's impact on system behaviour and performance across the full range of weather conditions. The difference in behaviour across seasons will be covered in this section. First, there are details on the observed behaviour of the SDAHU model and the DDAHU under fault-free conditions for two different seasons (Spring and Summer). In the subsequent section, the behaviour under a sample fault case will then be analysed in comparison to the previous baseline case. The outdoor air damper and cooling coil control are the focus of the analysis below. The fan speed will remain mostly constant across the annual dataset so it is not highlighted.

3.1. Baseline operation (SDAHU)

The first season analysed is Spring in which we expect to see milder outdoor air temperatures. This equates to maximum activity for the economizer and minimum cooling coil use. The OA damper control sequence can be seen in Figure 4 as being activated in the range of 3°C to 12.7°C (37.5°F to 55°F). The supply temperature setpoint is set at 55F, so the damper modulating to 100% is expected. Because the simulated range of this sample day never reaches the minimum or maximum thresholds for economizer mode (33°F, 60°F), we never see the minimum position of the damper of 10%. The cooling coil is modulated based on the SAT setpoint and works in conjunction with the OA damper in milder conditions. In Figure 4, we can see the OA damper is modulated to meet SAT setpoint until the OA temp reaches its maximum threshold of 60°F. The OA damper then is commanded to a minimum value of 10% while the cooling coil command signal is ramped up to meet the SAT setpoint at this instance. As

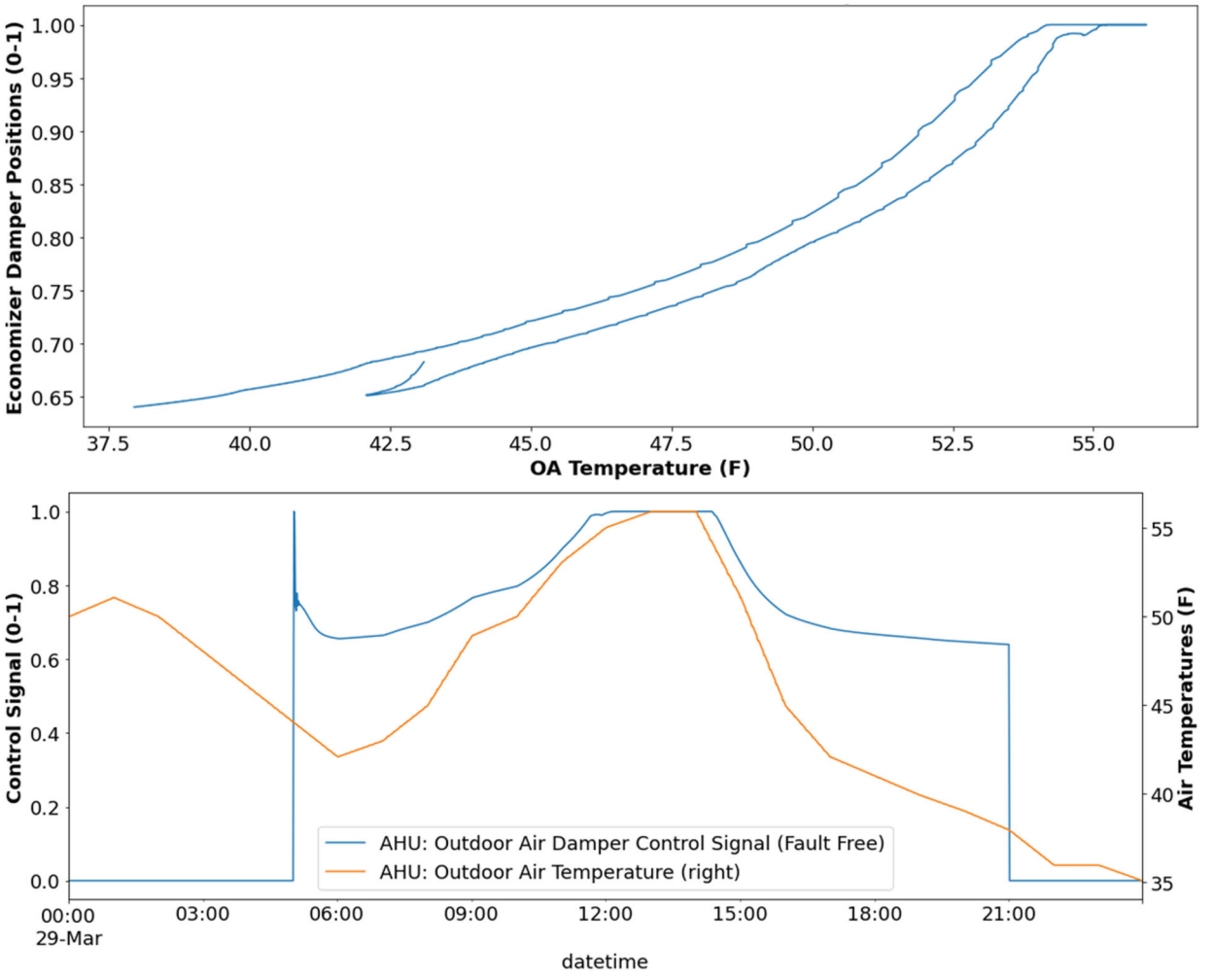

Figure 4. Validation of Economizer control sequence.

seen by the SAT plot in Figure 5, the setpoint of 55°F is always met. Analysing the SDAHU model's behaviour during the Summer period is relatively more straightforward compared to the nuanced operation of the OA damper during shoulder season, when economizing is frequent. As seen in Figure 5, during summer operation, the OA temperatures range at values greater than the 60°F maximum threshold for economizing, so the damper is always set at 10%, while the cooling coil is modulated instead to meet the SAT setpoint.

3.2. Baseline operation (DDAHU)

In the Spring season, the DDAHU is operated in the economizer mode or the mechanic cooling mode. First, we examined the weather conditions (i.e. OAT). This is a prerequisite to validate the system's operation mode because the OAT was used in the control sequence to drive the system's operation. For example, when the OAT is less than 15.6 °C (60 °F) and PI controller output is lower than 100, the system is operated under the economizer cooling mode. Under this mode, the cooling coil valve position is fully closed, and the OA damper is adjusted between 0% and 100% opening position. Secondly, we validated the control signal and actuator's responses to determine if the control logic was successfully carried out and if the actuator's response was correct. For example, under the fault-free operation, the coil valve position should follow the valve control signal, indicating that there is not a stuck valve fault. Thirdly, we inspect the responses in various process variables (e.g. SAT, air flow, and static pressure). For example, if the cooling coil valve position is increased to provide more cooling, the SAT should decrease. Lastly, we examined whether a holistic control objective is achieved during the system's operation. For instance, for the well-controlled system, the AHU SAT should meet the SAT setpoint and the zone temperature should reach the zone temperature setpoint.

Figure 6 illustrates the OAT, cooling coil valve and control signal on April 12. Figure 6 (left) illustrates the OA temperature, the OA damper control signal and the OA damper position. It can be seen that when the OA

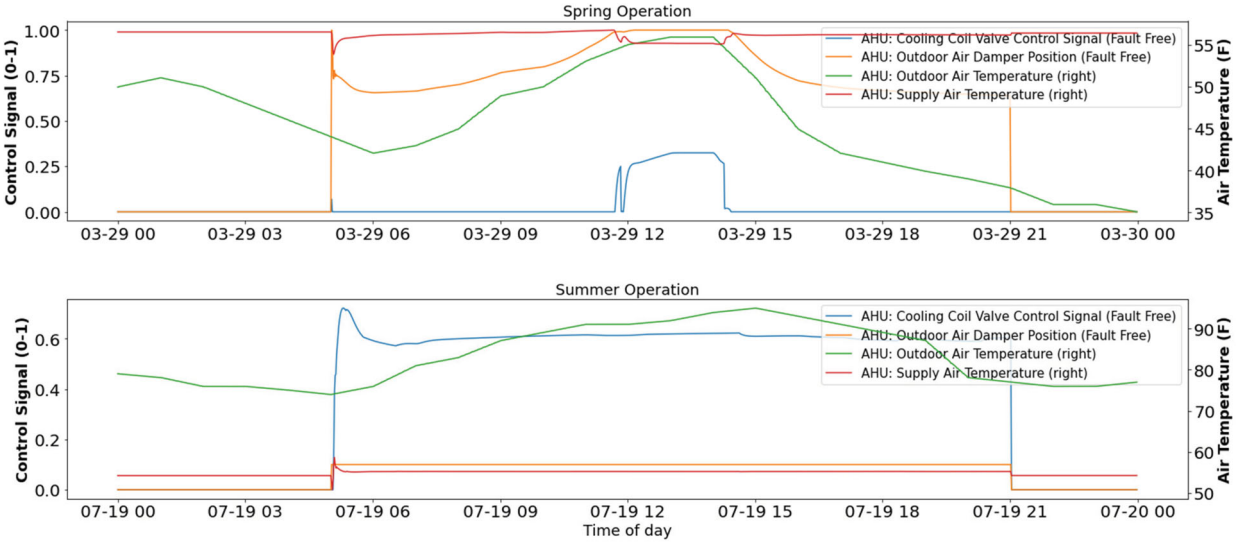

Figure 5. Comparison of Spring and Summer Operation of OA damper and cooling coil maintaining 55F supply temperature.

temperature is lower than 15.6 °C, the OA damper position is controlled to provide necessary cooling. Figure 6 (right) illustrates the cooling coil valve control signal and the valve position, as well as the cold deck SAT and setpoint. It can be seen that the cooling coil is fully closed during the occupied hours because the OA temperature is less than 15.6 °C. The cold deck SAT is well maintained around the setpoint in most of the occupied hours.

The validation scenario in the Summer season is the same as the process used in the Spring season. In the Summer season, the DDAHU is primarily operated in the mechanic cooling mode. In addition to the validation points in the Spring season, in the summer season, extra efforts were made to ensure the zone temperature was maintained around the cooling setpoint. Here, we use the operation on August 23 as an example. Figure 7 (Left) illustrates the OA temperature, the OA damper control signal and the OA damper position. It can be seen that when the OA temperature is higher than 15.6 °C, the OA damper position is controlled to the minimum position (28% of full openness). Figure 7 (Right) illustrates the cooling coil valve control signal and the valve position, as well as the cold deck SAT and setpoint. It can be seen that the cooling coil is adjusted to provide necessary

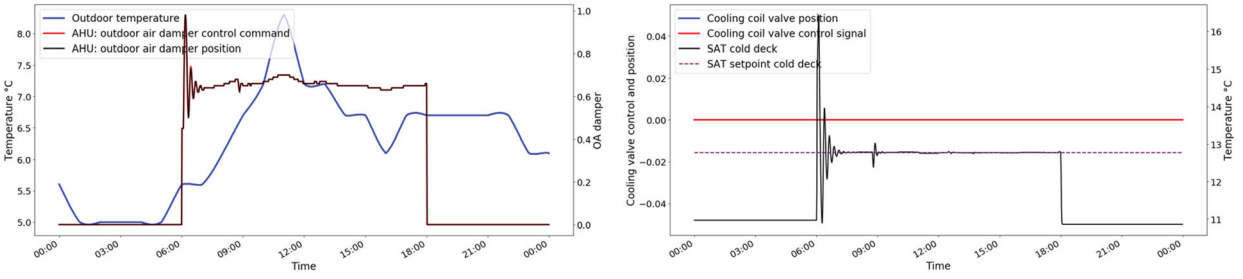

Figure 6. Left: OA temperature and OA damper; Right: cooling coil valve control signal, valve position, SAT and setpoint (date: April 12).

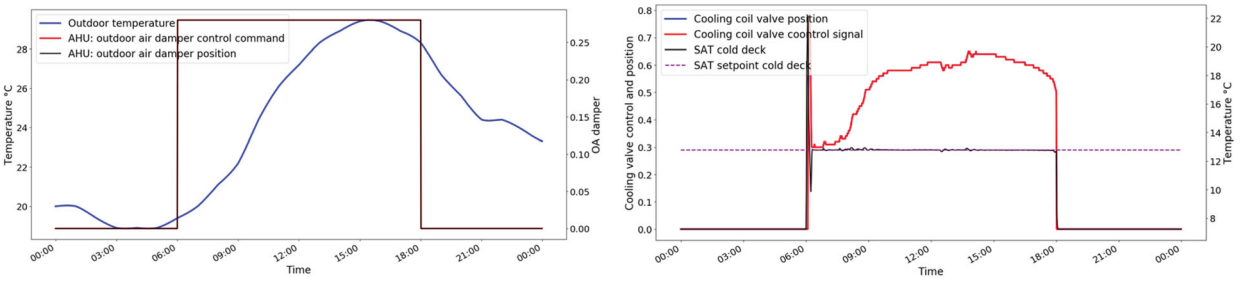

Figure 7. Left: OA temperature, and OA damper; Right:: cooling coil valve control signal, valve position, SAT and setpoint on the cold deck (date: August 23).

cooling during the occupied hours because the OA temperature is higher than 15.6°C. The cooling coil valve is well-controlled despite a short oscillation due to the controller tuning in the beginning of the system. The cold deck SAT is well maintained around the setpoint in the rest of the occupied hours.

3.3. Faulty operation (SDAHU) – OA damper stuck at minimum (10%)

For the faulty operation example, the outdoor air damper stuck at minimum case is presented. As seen in Figure 8, the same day is plotted as in Figure 5, although now we see the faulty operation of the damper during this fault. The first thing to observe is that the control signal is at 100% throughout the entirety of the day. This is caused primarily by the feedback loop of the controller, which calculates the difference between the mixed air temperature and the supply air setpoint of 55°F. As the temperature difference increases due to the stuck component, the control output is saturated at 100%. Meanwhile, the outdoor air damper ground-truth position is plotted at a constant value of 10%, which allows us to effectively validate the presence of our fault. This fault results in higher cooling coil activity and higher energy consumption due to the lost opportunity of economizing based on ideal weather conditions. This can be seen in the subsequent plot in Figure 8, in which the cooling coil signal is noticeably higher for the faulty case.

The presence and symptoms of each fault will not always be evident, based on the weather conditions and/or the operational state of the HVAC system. This is most evident in the Summer case for the OA Damper Stuck at Minimum case, as shown in Figure 8, where the OA temperatures reach their maximum range, up to 95°F. This is well beyond the maximum threshold for economizing, and as a result, the damper is already at minimum position. The lack of OA damper modulation means the faulty, and baseline cases are virtually indistinguishable from one another, as seen by the pair of Figures below, where the OA damper control signal overlaps at 10%, and the cooling coil control signal for both cases is also equivalent.

3.4. Faulty operation (DDAHU) – cooling coil valve stuck (80%)

When the cooling coil valve is stuck at a higher position, it causes the SAT to be lower than the normal operation, and excessive cooling will be provided. Figure 9 illustrates the faulty behaviour and the SAT. It can be seen that the coil valve stocks at 80% (i.e. 0.8 of the full position in the red line) compared to the normal position (i.e. 0 of the full position in the blue line). Consequently, the SAT is maintained around 9 °C (indicated in the purple line) instead of 13°C (indicated in the black dash line) as it should be in the fault-free operation condition.

Figure 10 shows another case example to demonstrate the fault symptoms under the cooling coil valve stuck fault in the DDAHU. When the cooling coil valve is stuck at 80% opening position, which is higher than the normal position, the coil valve position signal is frozen at 80% and the valve control signal reaches 0 to try to offset the

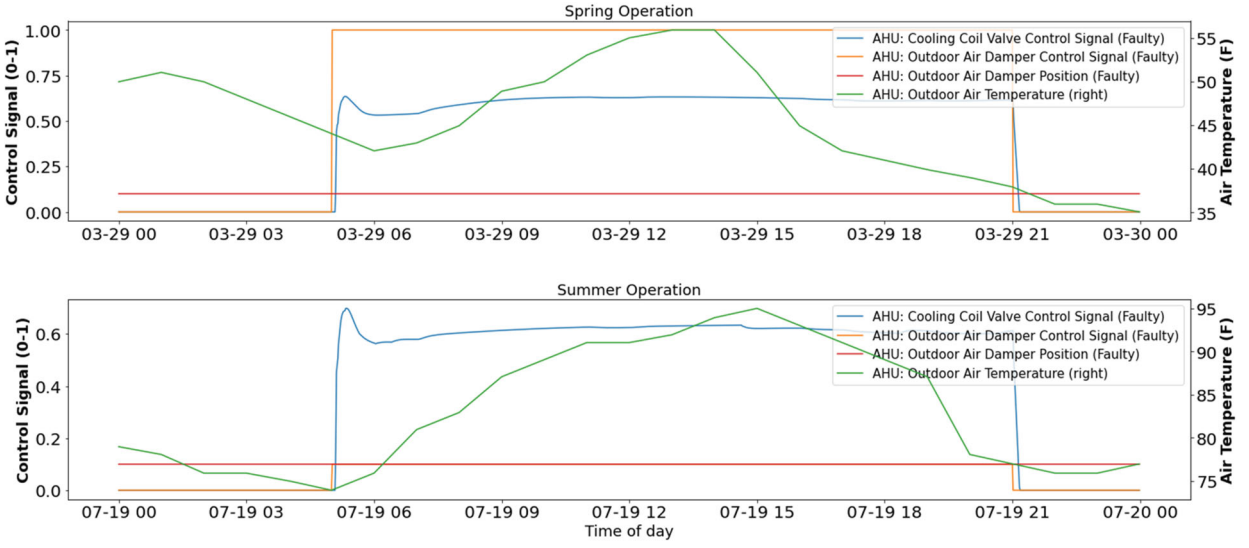

Figure 8. Spring operation of a stuck OA damper. Cooling coil is more active in faulted cases in order to maintain 55F supply temperature, summer operation of a stuck OA damper, the ambient conditions during summer cause the damper to stay at minimum and, therefore, the symptoms are not prevalent in this season.

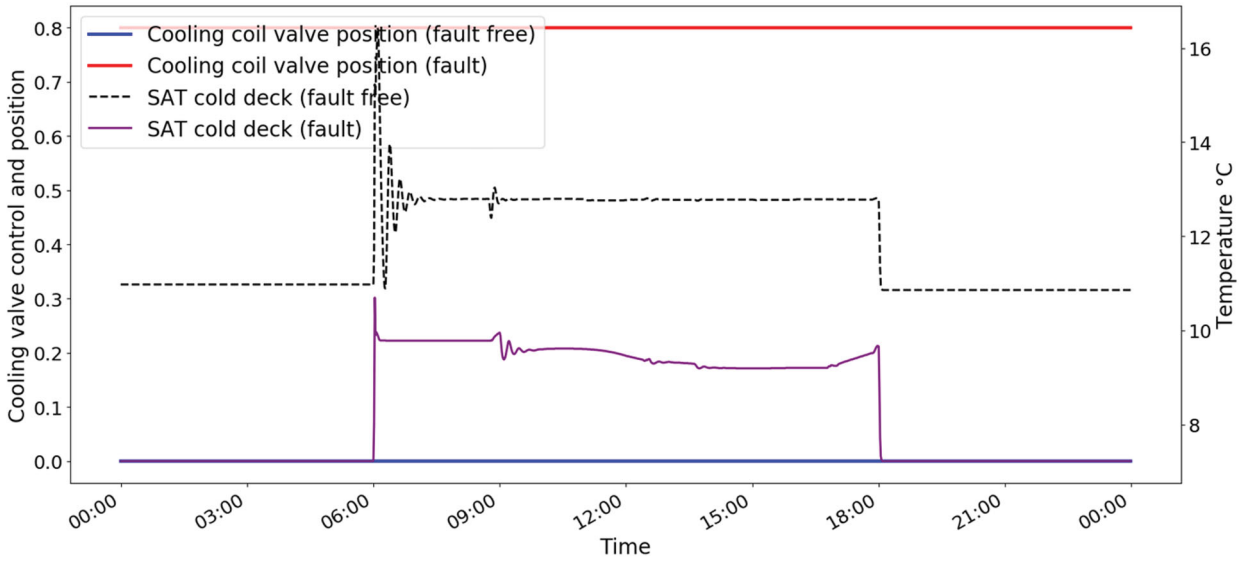

Figure 9. Spring operation: cooling coil valve control signal, valve position, SAT and setpoint on the cold deck (date: April 12).

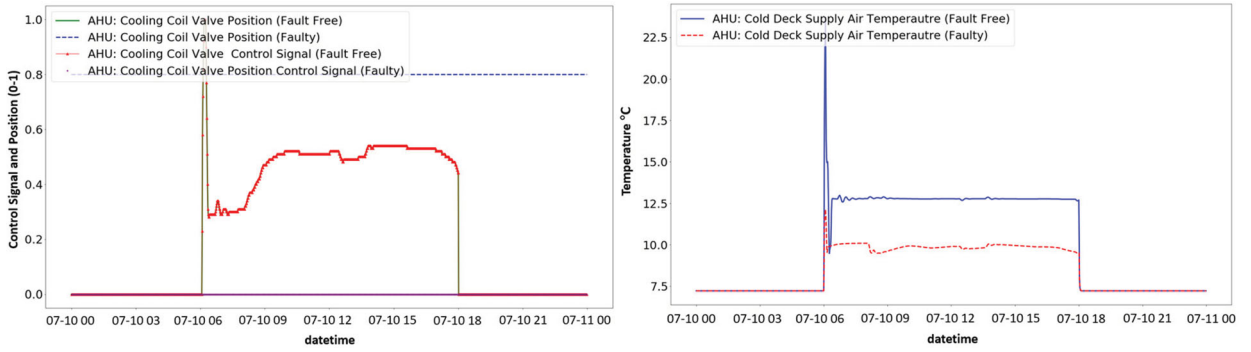

Figure 10. DDAHU fault symptom validation (cooling coil valve stuck at an 80% position fault). Left: coil control signal and position; Right: cold deck SAT.

effects of the higher coil valve position as shown in the left of Figure 10. However, because the cooling coil valve is out of control, this fault causes the SAT in the cold deck to be lower than the normal value (i.e. around 10°C instead of 13°C under the fault-free operation as given in the right of Figure 10). In addition, this fault causes the cascading abnormal operation in the downstream VAV terminal units.

4. Discussion

Creating the ground-truth verified operational data for the systems presented in this article was a significant effort that required a multi-year collaboration with multiple HVAC and modelling experts across a number of institutions. Several challenges were encountered, and resolving them generated a valuable set of insights for those seeking to leverage simulation models for system-level operational analytics and control applications. The associated lessons learned for each system type are presented to inform future efforts by other researchers, also looking to extend the application of building and system-level simulation models.

Casillas et al. 2020 detailed the protocol for creating the datasets by first conducting small-scale simulations and validation before proceeding to full-scale simulation. Individual control sequences are best tested in functional tests that can be executed in system models (i.e. HVACSIM+ or Modelica) but may lead to unintended behaviours as part of a full-scale model (co-simulation with EnergyPlus) with varying weather conditions and operational states. The protocol is particularly effective in validating documented control sequences across different seasons. Dedicating time to validating small-scale simulation results can avoid wasted time and resources, given that scaled-up annual simulations can take several days to complete and occupy anywhere between 1 and 10 GB of memory. The lessons learned are categorized and summarized in Table 4 below.

Table 4. Overview of lessons learned from AHU fault modelling and validation efforts.

Problem encountered	System affected	Impact on output	Lesson learned
Control sequence needs refinement	Coil, OA damper	Higher than expected cooling coil load, out of range values for incoming air temperatures	Add preheating, disable cooling coil until OA damper has reached 100% during economizing.
Inappropriate fault imposition method	Actuated components (damper, coil valve)	Mechanical component (valve and damper) control signals targeted without ground-truth data on actuator position	Add position variable to give the control signal the ability to behave according to its PID control loop output
Inappropriate sizing of components	Cooling and heating coils	SAT setpoint is met, zone-level comfort is negatively affected	Resize components based on observed load given climatic conditions and internal loads of the space conditioned by the system
Abnormal temperature behaviour during low flow conditions	Leaving coil temperature sensor measurements	Abnormal supply air temperatures	Create virtual bypass values that pass the incoming coil temperatures through the coil without heat transfer calculations applied.
Time mismatch during Co-simulation	Occupied and occupied modes	Mismatched operating schedules	Disable daylight savings in IDF file

4.1. Control sequence refinement

Compared with the previously mentioned fault model validation protocol, in which a few days were selected and only employed, it is necessary to add control sequences, which enable a holistic representation of a properly controlled building under all operational conditions. For example, in the DDAHU control, freezing protection functionality was added after encountering an issue during winter operation. In the original DDAHU model, there was no freezing protection control sequence during the unoccupied hours when the system was completely shut off. This caused the SAT to be extremely low (e.g. as low as 10 F) when the OAT was low in the winter season. In the real system, the freezing protection control sequence may be adopted even when the system is switched to the unoccupied mode (i.e. the system does not provide the desired cooling or heating during unoccupied hours). The freezing protection sequence often enables the preheating or triggers the freezing alarm so that the operators can fix the fault quickly. This issue may only occur when whole year simulation is performed to enable the system control simulation to mimic this operating condition.

In addition to issues experienced in the DDAHU model, there were some inconsistencies between the control sequence programmed in the model and the best practices that we caught during our validation process. The model has two PID control loops, one for the economizer control and one for the cooling coil valve control. The economizer control uses the mixed air temperature as the control variable while the SAT controls the second loop. The problem occurs when economizing is enabled during mild conditions. Both control loops compete against each other to satisfy their setpoints, which leads to cooling while the outdoor air damper is modulating. Best practice prescribes the cooling coil valve stay disabled until the economizer output is 100%. Modulating the cooling coil valve before this condition results in unnecessary energy consumption and does not allow the economizer to take full advantage of ideal outdoor air conditions. These types of interconnected control loops need to be programmed in sequence so that the cooling coil valve control is disabled in economizing mode until the outdoor air damper reaches 100% open position.

4.2. Component sizing

Improper component sizing in the component model may significantly affect an accurate evaluation of the system's behaviours under fault-free and faulty conditions. In addition, the improper sizing of a component may not only be noticeable when evaluating an individual component's performance but becomes more critical when assessing fault's effects during system-level fault simulations. For example, in the DDAHU simulation, the system model, which was developed in HVACSIM+ software, consists of various component models (i.e. coils, valves and dampers) in the system. If the heating coil is downsized in the model, this can cause a lower SAT even if the coil valve is fully opened during Winter's operation. This further affects the assessment of the system's behaviours under faulty operations. For example, the stuck heating coil valve fault (at a higher position), or the heating coil fouling fault cases modelled for the DDAHU may not cause significant fault symptoms (e.g. observable higher SAT compared with the baseline) if the heating coil is downsized. Therefore, properly setting model parameters to avoid component sizing issues at the system-level simulation should be paid more attention.

4.3. Fault imposition methods

When imposing actuator-related faults (e.g. a damper stuck fault), the changed value should be injected to

freeze the actuator action, but not fix the control signal. This is because, in the real practice, the s tuck actuator is believed to be some mechanical/communication issues (e.g. the linkage between the driver and actuator is broken, or the communication between the DDC and the drive is lost). The DDC should output the proper control signal to compensate/tolerate the fault. Therefore, the control signal should not be frozen but instead, the actuator position to ensure that the control signal is calculated by the existing PID loop in response to the growing error caused by the stuck actuator. To address this issue, some extra points (i.e. ground-truth valve position feedback) should be added to the original equipment model to mimic the control behaviour and simulate the fault effects.

4.4. Low flow conditions

A common occurrence for the Modelica-based model is indeterminate conditions when fluid mass flows appro ach zero, referred to here as 'low flow conditions'. This happens often during overnight scenarios, in which the flow provided to a water coil or the airflow approaches zero due to the lack of demand in the system in unoccupied hours. This low flow causes abnormal conditions which manifest in different ways during modelling. One example is its effects on SAT during severe damper fault cases. In reality, when the temperature of the air is too low (less than the temperature of the inlet water), it is possible that it 'absorbs' heat from the cooling coil. In simulation, the process for calculating the water temperature in a heat exchanger becomes unreliable when the water flow is approaching 0. Low flow conditions can also cause abnormal temperature deviations and flat profiles given the limitations of the sensor modules we use during simulations. These flat temperatures may have effects on their associated control loops, for instance, the SAT control loop sends a cooling coil valve control signal of 100% due to the flat measurement of the SAT sensor when the supply airflow is zero.

Similarly, when examining HVACSIM+, we found that low flows can also introduce numerical challenges. Besides singularity issues that may arise given near-zero values, the intricacies of solving nonlinear equations in such conditions can sometimes yield multiple potential solutions. For instance, during the simulation of a mixing box (TYPE 325) in HVACSIM+ under a low flow condition, both a slight positive and a slight negative outdoor air mass flow rate could be deemed acceptable, largely due to the minimal variation in outdoor air damper differential pressure during the solution search. Without a proper handle, such scenarios may cause the simulation to oscillate between these possible solutions, leading to non-convergence or crash of the simulation. However, it is vital to recognize that the precision of results under low flow is not the primary concern given their negligible magnitude. What is crucial is ensuring numerical stability throughout the simulation. Thus, implementing a low flow protection mechanism (e.g. the absolute value of the mass flow rate cannot be lower than 5e-4) can be invaluable, as it directs the simulation solver to consistently select a stable solution, guaranteeing simulation robustness.

4.5. Co-simulation

Another consideration is related to co-simulation frameworks such as the one presented here for the SDAHU models. The change of data between the EnergyPlus idf file FMU and the AHU system models is not only limited to building thermal loads but also used to determine when the building is in Occupied or unoccupied mode. The documented occupied times of 6pm to 10pm are scheduled in the FMU, and the occupied output is fed to the model as a Boolean value. The problem observed during validation is related to the daylight savings time option in the idf file being set to true, which meant that the start of daylight savings time resulted in a 1-hr shift in time reporting from the FMU. This manifests in the model as an occupied time of 5am to 9pm, which is inconsistent with the provided documentation.

The model validation under all operational conditions was also applied to the equipment physical model validation to ensure the equipment model accurately outputs values. For example, in the simulated cooling valve model, the operating position limit should be set to 100 (i.e. fully opened) as the maximum value even though the cooling supply may not be enough in extremely hot weather. After encountering this issue, all the actuator models were re-examined to add the actuator operating position limit.

5. Conclusion

In this study, we detailed the methods and results from generating a comprehensive fault dataset for 2 types of AHU systems, which amount to 75 total fault cases with 3.7 billion data points. The lessons learned from applying simulation models in this way can assist other researchers seeking to use models to reflect a wide range of realistic system operations. The lessons learned covered in this study illustrate the state of high-fidelity models and their use for building operational applications as opposed to model-based design. As HVAC models become more detailed and representative of real systems, it is important to take into account the methods

by which real applications, such as FDD, process HVAC system data. Some of the pitfalls experienced in modelling faults in these systems are addressable through the methods offered in this study but also through new developments in modelling software. For instance, the recently released Spawn of Energy Plus brings a new co-simulation framework that passes a limited list of parameter settings through the functional mockup unit, and thus, removes the need for accounting for daylight savings adjustments.

Moving forward, the same method of building fault models and datasets can be applied to additional systems, such as packaged and split heat pump systems, which are likely to see an increased prevalence in our building stock given federal investments in electrification. These systems will benefit from robust FDD algorithms to ensure they are performing at rated efficiencies and delivering value to consumers. Future work can also explore how fault models can be incorporated into virtual platforms such as BOPTest (Blum et al. 2021), designed to evaluate the performance of HVAC control algorithms. Integration of these fault models opens the door to control design and assessment while considering the presence of common faults. Additionally, we plan to extend this fault study to characterize fault behaviour under additional common control strategies (i.e. ASHRAE Guideline 36). Furthermore, the FDD datasets will enable further benchmarking of FDD algorithm performance and can characterize the effectiveness of industry-recommended fault rules such as those found in ASHRAE Guideline 36. Through detailed fault modelling and simulation of the system's faulty operation, we efficiently assess a system's control robustness or fault tolerance. That is to say, when we inject faults (with different severity levels) into the system, we can evaluate whether the control objectives can be met.

Acknowledgement

This work was supported by the Assistant Secretary for Energy Efficiency and Renewable Energy, Building Technologies Office, of the U.S. Department of Energy under Contract No. DE-AC02-05CH11231. We also recognize each of the fault detection and diagnostic tool developers who participated in this survey. We would also like to thank Brian Walker and the Building Technologies Office as well as our data contributors.

Disclosure statement

No potential conflict of interest was reported by the author(s).

Funding

This work was supported by the Assistant Secretary for Energy Efficiency and Renewable Energy, Building Technologies Office of Energy Efficiency and Renewable Energy, of the U.S. Department of Energy under Contract No. DE-AC02-05CH11231.

Data availability statement

The data that support the findings of this study are openly available at https://faultdetection.lbl.gov/data/

ORCID

Zhelun Chen http://orcid.org/0000-0002-5570-1264

References

Andriamamonjy, A., D. Saelens, and R. Klein. 2018. "An Auto-Deployed Model-Based Fault Detection and Diagnosis App roach for Air Handling Units Using BIM and Modelica." *Automation in Construction* 96:508–526. https://doi.org/10.1016/j.autcon.2018.09.016.

ASHRAE. 2020. *ASHRAE Handbook-Systems & Equipment, Chapter 12*. Atlanta: American Society of Heating Refrigeration and Air Conditioning Engineers, Inc.

Blum, D., J. Arroyo, S. Huang, J. Drgoňa, F. Jorissen, H. Taxt, Y. Chen, K. Benne, D. Vrabie, and M. Wetter. 2021. "Building Optimization Testing Framework (BOPTEST) for Simulation-Based Benchmarking of Control Strategies in Buildings." *Journal of Building Performance Simulation* 14 (5): 586–561. https://doi.org/10.1080/19401493.2021.1986574.

Bushby, S. T., and C. Park. 2001. Using the Virtual Cybernetic Building Testbed and FDD Test Shell for FDD Tool Development NISTIR 6818.

Casillas, A., G. Lin, and J. Granderson. 2020. "Curation of Ground-Truth Validated Benchmarking Datasets for Fault Detection & Diagnostics Tools." *Proceedings of the 2020 ACEEE Summer Study on Energy Efficiency in Buildings*.

Chen, Y., G. Lin, E. Crowe, and J. Granderson. 2021. "Development of a Unified Taxonomy for HVAC System Faults." *Energies* 14 (17): 5581. https://doi.org/10.3390/en14175581.

Clark, D. R., and W.B. May. 1985. *"HVACSIM+ Building Systems and Equipment Simulation Program - User's Guide." PB-86-130614/XAB; NBSIR-85/3243*. Washington, DC: National Bureau of Standards, Building Equipment Division.

Deru, M., K. Field, D. Studer, K. Benne, B. Griffith, P. Torcellini. 2011. U.S. Department of Energy Commercial Reference Building Models of the National Building Stock. (February 2011).

Fernandez, N., S. Katipamula, M. Zhao, W. Wang, Y. Xie, and C. Corbin. 2017. Impacts on commercial building controls on energy savings and peak load reduction. Pacific Northwest National Laboratory. PNNL Report Number PNNL-25985.

Granderson, J., G. Lin, D. Blum, S. Earni, J. Page, and M.A. Piette. 2017. Optimizing Operational Efficiency: Integrating Energy Information Systems and Model-Based Diagnostics. https://doi.org/10.20357/B7988J

Granderson, J., G. Lin, A. Harding, P. Im, and Y. Chen. 2020. "Building Fault Detection Data to aid Diagnostic Algorithm Creation and Performance Testing." *Scientific Data* 7 (1): 1–14. https://doi.org/10.1038/s41597-020-0398-6.

House, J. M., H. Vaezi-Nejad, and J. M. Whitcomb. 2001. An Expert Rule Set for Fault Detection in Air-Handling Units. ASHRAE Winter Meeting CD, Technical and Symposium Papers, 1005–1018.

Huang, S., Chen, Y., Ehrlich, P., & Vrabie, D. (2018). A Control-Oriented Building Envelope and HVAC System Simulation Model for a Typical Large Office Building. *Proceedings of*

2018 Building Performance Modeling Conference and SimBuild, 729–736.

Huang, S., W. Zuo, D. Vrabie, and R. Xu. 2021. "Modelica-based System Modeling for Studying Control-Related Faults in Chiller Plants and Boiler Plants Serving Large Office Buildings." *Journal of Building Engineering* 44: 102654. https://doi.org/10.1016/j.jobe.2021.102654.

Kramer, H., G. Lin, C. Curtin, and J. Granderson. 2020. Proving the Business Case for Building Analytics Energy Technologies Area October. https://doi.org/10.20357/B7G022

Li, S. and J. Wen. 2010. Development and Validation of a Dynamic Air Handling Unit Model - Part I (RP 1312), ASHRAE Transactions 116 (Pt. 1): 45–56.

Li, S., J. Wen, X. Zhou, and C. J. Klaassen. 2010. "Development and Validation of a Dynamic Air Handling Unit Model - Part II (RP 1312)." *ASHRAE Transactions* 116 (Pt 1) 57–73.

Liao, H., W. Cai, F. Cheng, S. Dubey, and P. B. Rajesh. 2021. An Online Data-Driven Fault Diagnosis Method for Air Handling Units by Rule and Convolutional Neural Networks.

Lin, G., H. Kramer, and J. Granderson. 2020. "Building Fault Detection and Diagnostics: Achieved Savings, and Methods to Evaluate Algorithm Performance." *Build. Environ* 168:106505. https://doi.org/10.1016/j.buildenv.2019.106505

Montazeri, A., and S. M. Kargar. 2020. "Fault Detection and Diagnosis in air Handling Using Data-Driven Methods." *Journal of Building Engineering* 31: 101388. https://doi.org/10.1016/j.jobe.2020.101388.

Park, C., D. R. Clark, and G. E. Kelly. 1986. *"HVACSIM+ Building Systems and Equipment Simulation Program: Building-Loads Calculation." PB-86-189909/XAB; NBSIR-86/3331*. Washington, DC: National Bureau of Standards.

Roth, K., D. Westphalen, L. Patricia, and M. Feng. 2004. "The Energy Impact of Faults in U.S. Commercial Buildings." In *International Refrigeration and Air Conditioning Conference*. West Lafayette, IN: Purdue University.

Schein, J., and S. T. Bushby. 2006. "A Hierarchical Rule-Based Fault Detection and Diagnostic Method for HVAC Systems." *HVAC&R Research* 12 (1): 10–12. https://doi.org/10.1080/10789669.2006.10391170

Wang, Shengwei, and Fu Xiao. 2004. "AHU Sensor Fault Diagnosis Using Principal Component Analysis Method." *Energy and Buildings* 36 (2): 147–160. https://doi.org/10.1016/j.enbuild.2003.10.002.

Wen, J., S. Pourarian, X. Yang, and X. Li. 2015. NIST 10D243 Tools for Evaluating Fault Detection and Diagnostic Methods for HVAC Secondary Systems of a Net Zero Building. National Institute of Standard & Technology. U.S. June 2015.

Wu, S., and J. Sun. 2012. "A Physics-Based Linear Parametric Model of Room Temperature in of Fi Ce Buildings." *Building and Environment* 50:1–9. https://doi.org/10.1016/j.buildenv.2011.10.005.

Yan, R., Z. Ma, Y. Zhao, and G. Kokogiannakis. 2016. "A Decision Tree Based Data-Driven Diagnostic Strategy for air Handling Units." *Energy & Buildings* 133:37–45. https://doi.org/10.1016/j.enbuild.2016.09.039.

Yu, Y., D. Woradechjumroen, and D. Yu. 2014. "A Review of Fault Detection and Diagnosis Methodologies on air-Handling Units." *Energy & Buildings* 82:550–562. https://doi.org/10.1016/j.enbuild.2014.06.042.

Yun, W., W. Hong, and H. Seo. 2021. "A Data-Driven Fault Detection and Diagnosis Scheme for air Handling Units in Building HVAC Systems Considering Undefined States." *Journal of Building Engineering* 35:102111. https://doi.org/10.1016/j.jobe.2020.102111.

Zhao, Y., J. Wen, and S. Wang. 2015. "Diagnostic Bayesian Networks for Diagnosing Air Handling Units Faults – Part II: Faults in Coils and Sensors." *Applied Thermal Engineering* 90:145–157. https://doi.org/10.1016/j.applthermaleng.2015.07.001.

Zhao, Y., J. Wen, F. Xiao, X. Yang, and S. Wang. 2017. "Diagnostic Bayesian Networks for Diagnosing Air Handling Units Faults – Part I: Faults in Dampers, Fans, Filters and Sensors." *Applied Thermal Engineering* 111:1272–1286. https://doi.org/10.1016/j.applthermaleng.2015.09.121.

Zhong, C., K. Yan, Y. Dai, N. Jin, and B. Lou. 2019. "Energy Efficiency Solutions for Buildings: Automated Fault Diagnosis of Air Handling Units Using Generative Adversarial Networks." *Energies*, 12 (3): 1–11. https://doi.org/10.3390/en12030527.